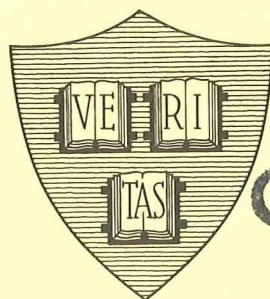


NASA CR-107453

EXPERIMENTAL INVESTIGATIONS ON THE IMPEDANCE BEHAVIOR OF A SHORT, CYLINDRICAL ANTENNA IN A LOSSY MAGNETOPLASMA

By

Bharathi Bhat and B. Rama Rao



CASE FILE
COPY

Scientific Report No. 2

February 1969

"Reproduction in whole or in part is permitted by the U. S.
Government. Distribution of this document is unlimited."

NATIONAL AERONAUTICS AND SPACE ADMINISTRATION

Prepared under Grant NGR 22-007-056

Division of Engineering and Applied Physics
Harvard University • Cambridge, Massachusetts

EXPERIMENTAL INVESTIGATIONS ON THE IMPEDANCE
BEHAVIOR OF A SHORT, CYLINDRICAL ANTENNA IN A
LOSSY MAGNETOPLASMA

by

Bharathi Bhat and B. Rama Rao

Scientific Report No. 2

Reproduction in whole or in part is permitted by the U. S.
Government. Distribution of this document is unlimited.

February 1969

Prepared under Grant NGR 22-007-056
Division of Engineering and Applied Physics
Harvard University, Cambridge, Massachusetts

for

NATIONAL AERONAUTICS AND SPACE ADMINISTRATION

EXPERIMENTAL INVESTIGATIONS ON THE IMPEDANCE BEHAVIOR OF A SHORT,
CYLINDRICAL ANTENNA IN A LOSSY MAGNETOPLASMA

BY

BHARATHI BHAT AND B. RAMA RAO

GORDON MCKAY LABORATORY, HARVARD UNIVERSITY

CAMBRIDGE, MASSACHUSETTS 02138

ABSTRACT

Experimental investigations have been made to determine the behavior of a short, cylindrical antenna at the refractive index resonance and cut-off regions of a cold, lossy magnetoplasma. The static magnetic field is oriented parallel to the axis of the antenna. The experimental results have been compared with the theories proposed by several authors. Of particular interest is the series of resistance maxima noticed at discrete frequencies corresponding to the cut-off and upper-hybrid resonance conditions. The significance of these results in interpreting the maxima in cosmic noise intensities and the "resonance spikes" observed in the ionograms of top-side sounder satellites has been discussed. The possibility of using such an antenna as a diagnostic probe for measuring electron-densities of over-dense magnetoplasmas has been indicated.

I. INTRODUCTION

A knowledge of the impedance behavior of dipole antennas radiating inside a magnetoionic medium is necessary for accurately interpreting the data obtained from diagnostic and propagation experiments performed in the ionosphere and outer space using rockets and satellites. The practical significance of this problem has prompted a number of theoretical papers describing the radiation characteristics of antennas immersed in magnetized plasmas; as the literature on this topic is quite vast only these papers which are relevant to this investigation will be mentioned here. For the most part these theoretical investigations are based either on quasi-static approximation¹⁾ or on an **uniaxial** type approximation (strong magnetic fields limit)^{2, 3)} with an assumed current distribution on the antenna. The very nature of these approximations precludes the consideration of antenna behavior for all ranges of the magnetoplasma parameters and especially near the resonance and cut-off conditions where the most interesting ionospheric phenomena manifest themselves. The antenna behavior at these critical frequencies is also conspicuously different from that in free space. Near resonance the refractive index of the characteristic wave becomes infinity thereby causing the antenna dimensions to become large in comparison with the characteristic wavelength. The quasi-static approximation becomes invalid in this region and the actual current distribution on the antenna will also differ significantly from the simple triangular distribution assumed in the analysis. In the uniaxial approximation it is assumed that the off-diagonal term of the permittivity tensor characterising the magnetoplasma is small in comparison with the leading diagonal term, which is true only when the applied static magnetic field is very large. When the plasma parameters approach cut-off however, the value of the off-diagonal term increases rapidly and becomes equal in magnitude to the leading diagonal term causing the

refractive index of one or the other of the characteristic waves to become zero. As will be explained later in this paper, the analysis of Lee and Lo⁴⁾ and Aoki³⁾ have shown that the simple triangular current distribution is again inadequate for predicting impedance behavior of the antenna under such conditions. The difficulty in the analysis and the doubts regarding the validity of the theoretical formulation at these critical regions underscores the need for more experimental investigations. Relatively few meaningful experiments under carefully controlled laboratory conditions have been performed to examine the behavior of a cylindrical dipole antenna in a magnetoplasma. Balmain¹⁾ has reported some laboratory measurements but his experimental results are ambiguous as they do not show any unusual behavior in the impedance at upper-hybrid resonance¹⁾ or at the cut-off frequencies probably due to the relatively high collision frequency in his experiments. Stone, Alexander and Weber^{5a,b)} Molozzi and Richardson⁶⁾ and Hugill⁷⁾ have made "in-flight" impedance measurements on a short dipole mounted on a rocket for certain ranges of magnetoionic parameters existing in the ionosphere; they have not, however, considered behavior at cut-off. The advantage of laboratory experiments over "in-flight" measurements is that in the former case the plasma parameters can be varied over a wide range, permitting accurate measurements at various conditions corresponding to cut-off and resonance; alternative diagnostic measurements can be made to determine the electron density, electron temperature and collision frequency as well as the strength and orientation of the applied magnetic field so that the prevailing experimental conditions are more precisely defined than is possible in rocket and satellite "in-flight" experiments.

This paper describes some laboratory investigations on the impedance characteristics of an electrically short cylindrical antenna inside a magnetized plasma with the static magnetic field applied parallel to the axis of the

antenna. The U. R. S. I. symbols $X = \frac{\omega_p^2}{\omega^2}$, $Y = \frac{\omega_c}{\omega}$, $Z = \frac{\nu_c}{\omega}$ and $U = 1 - jZ$ will be used to describe the plasma parameters, where $\omega_p = \sqrt{\frac{n_0 e^2}{m \epsilon_0}}$ = angular plasma frequency, $\omega_c = \frac{eB_0}{m}$ = angular cyclotron frequency, ν_c = collision frequency and ω = angular signal frequency of the antenna. B_0 is the axial static magnetic field and n_0 is the electron density and m and e are the electron mass and charge respectively. For clarification, the notation of Stix⁸⁾ will be used for identifying the various cut-off's and principal resonances of the magnetoplasma. The variation in the input impedance of the antenna will be studied at transition regions described by the following plasma parameters for a one-component, loss-less plasma: 1) upper hybrid resonance where $X = 1 - Y^2$ ($S = 0$), 2) electron cyclotron resonance where $Y = 1$ ($R = \infty$) and 3) the cut-off conditions given by $X = 1$ ($P = 0$), $X = 1 + Y$ ($L = 0$) and $X = 1 - Y$ ($R = 0$). The Stix symbols⁸⁾ P , R , L , and S for one one-component plasma are given by $P = 1 - X$, $R = 1 - \frac{X}{1 - Y}$, $L = 1 - \frac{X}{1 + Y}$ and $S = \frac{1}{2} (R + L)$. The conditions $R = 0$, $L = 0$, $P = 0$, $R = \infty$ and $S = 0$ constitute the boundary surfaces on the CMA diagram for a one-component plasma given in Fig. 5; these surfaces divide the diagram into various regions which will be convenient for later discussion of wave-propagation phenomena in the plasma.

II. EXPERIMENTAL APPARATUS

The experimental investigations were made in a hot-cathode, Helium d.c. discharge tube 38cm in length and 6.5cm in diameter. The positive column of the discharge was placed along the axis of a solenoid 28cm long and 15cm in diameter. The antenna was a copper rod 4mm in diameter and 3.5cm long. Since the length of the antenna was very short compared to the wavelength of the highest signal frequency used in the experiment ($\frac{h}{\lambda_0} = 0.07$ at 600 MHz), its radiation field is negligible and the plasma discharge around the antenna has

a significant effect only on the reactive near field of the antenna. Hence the finite size of the plasma container does not seriously compromise the "infinite plasma" assumption made in the theoretical analysis.

The antenna was connected to the inner conductor of a vacuum-tight precision coaxial connector; this eliminates large junction effects near the driving point of the antenna. The coaxial connector was mounted at the center of a copper disc which also serves as the anode of the discharge tube. The longitudinal magnetic field in the solenoid was measured by a Hall probe and the antenna was placed in the uniform magnetic field region at the center of the solenoid. A transistorized magnet power supply with a current regulation of one part in 10^5 and with a precision control for fine magnetic field adjustments was used in the experiments. The effect of a magnetic field parallel to the axis of the positive column of a d.c. discharge has been investigated by many authors⁹⁾. The principal effect of the magnetic field is to confine the electrons within a Larmor radius and reduce radial diffusion to the walls of the plasma vessel; this effect causes a slight increase in the electron density and a decrease in the electron temperature. The glow region is brighter at the center than at the walls and the effect is more marked at lower neutral gas pressures. The electron density in the plasma container could be controlled by varying the discharge current. A constant current regulator was used in series with d.c. power supply to the plasma tube; this ensured that the discharge current (hence electron density) remained at a constant value throughout the experiment. Any increase in the electron density caused by an increase in the solenoid magnetic field was immediately compensated for by the regulator through a decrease in the d.c. potential to the discharge. This regulation was good for low to moderate magnetic fields used in the experiment, but broke down for higher fields. The influence of the magnetic field on the electron density profile has been

measured by Bickerton and Von Engel¹⁰⁾. The antenna is placed at the axis of the discharge tube where the electron density is at maximum; it has not been possible to estimate the effect of the radial density variation on the antenna behavior although it is likely to cause a smearing of the sharp resonances in the resistance and the reactance observed at certain frequencies.

The electron density and electron temperature of the plasma were determined by a planar Langmuir probe. The probe was made out of a 2.4mm diameter tungsten wire sheathed in glass with only the flat end exposed to the plasma. The accuracy of the diagnostic measurements of magnetoplasmas using Langmuir probes are subject to criticism because of difficulty in interpreting the results. However, improved versions of this model have been developed by Bickerton and Von Engel¹⁰⁾ and by Heald and Wharton¹¹⁾ for an approximate determination of electron temperatures and densities. The electron neutral collision frequency $\nu_{en} = 2.66 \times 10^{22} \sqrt{T_e} Q_m P$ was determined from the collision cross-section for helium measured by Golden and Bandel¹²⁾. In the above equation T_e = electron temperature of the plasma in degrees Kelvin, P = neutral gas pressure in mm of Hg and Q_m = electron neutral collision cross-section for momentum transfer in cm^2 . Since the plasma is weakly ionized it is assumed that the electron-ion collisions are negligible, so that $\nu_c \approx \nu_{en}$. The static magnetic field or the signal frequency of the antenna was varied so that the refractive index of the plasma corresponded to the resonance and cut-off conditions which were mentioned earlier. The collision frequency was varied principally by changing the neutral gas pressure of the helium in the discharge. A schematic diagram of the experimental apparatus is shown in Fig. 7.

III. IMPEDANCE BEHAVIOR AT UPPER HYBRID AND ELECTRON CYCLOTRON RESONANCE

Within the quasi-static limit and for an assumed triangular type of current

distribution on the antenna the input impedance Z_A of a short cylindrical antenna in an axial magnetic field has been derived by Balmain¹⁾:

$$Z_A = R_A + jX_A = \frac{1}{j2\pi\epsilon_0 \omega h K'} \left[\ln \frac{h}{a} - 1 + \ln \sqrt{K'/K_0} \right] \quad (1)$$

where R_A and X_A are the input resistance and reactance of the antenna. h and a are the length and radius of the antenna, $K' = 1 - \frac{XU}{U^2 - Y^2}$ and $K_0 = 1 - \frac{X}{U}$; ϵ_0 is the permittivity of free space.

Galejs²⁾ has used a variational method with a two-term sinusoidal type trial function for the antenna current and obtained a similar expression in the quasi-static limit as Balmain's. In the limit of no collisions when $Z = v_c/\omega = 0$, it is seen from Eqn. 1 that for $X < 1$ and $Y^2 < 1$ the antenna impedance will have a resistive component for $Y^2 > 1 - X$. The input resistance reaches infinity at the hybrid resonance frequency $Y^2 = 1 - X$ ($S = 0$) and drops to zero for $Y^2 < 1 - X$. For small but finite losses $Z \ll 1$ the resistance goes through a finite maximum near upper hybrid resonance. Similarly near electron cyclotron resonance $Y = 1$ ($R = \infty$), Eqn. 1 indicates that the probe reactance reaches a sharp minimum causing a corresponding peaking in the conductance. The quasi-static approximation becomes invalid at cyclotron resonance necessitating large correction terms in the theory as indicated by Balmain¹⁾. Seshadri¹³⁾ has recently considered the impedance behavior of an infinitely long cylindrical antenna in the resonant region of a magnetoplasma. The axial component of the antenna current I_z near the driving point as derived by him is given by:

$$I_z = c \ln \left(\frac{1}{z} \right) \sqrt{\frac{(1-X)(1-Y^2-X)}{1-Y^2}} \quad (2)$$

where c is a constant whose value depends on the antenna radius. From this formula it is seen that $I_z = 0$ when $X = 1 - Y^2$ or $X = 1$ and $I_z = \infty$ when $Y = 1$;

correspondingly the impedance reaches infinity at the upper-hybrid resonance and plasma cut-off, and zero at the cyclotron resonance.

Figures 1, 2, and 4 show the measured impedance and admittance of the antenna for various plasma conditions. The experiments reported in Figures 1 and 2 were performed at a fixed signal frequency of 600 MHz and the applied d.c. magnetic was varied for a fixed value of the plasma frequency. In Fig. 4 the signal frequency was varied from 120 to 480 MHz, while the plasma frequency and the d.c. magnetic field were kept at a constant value. The loci of the experimental parameters corresponding to Figures 1, 2, and 4 are shown on the CMA diagram in Fig. 5. It is seen that each of these loci intersect the boundary surfaces $X = 1 - Y^2$ ($S = 0$) and $Y = 1$ ($R = \infty$) corresponding to the upper-hybrid and cyclotron resonance conditions respectively. Fig. 1 shows the results of the experiment performed at a neutral gas pressure of 50 μ Hg. The electron density measured by the Langmuir probe for zero magnetic field gave a plasma frequency of 320 MHz. The electron temperature T_e was 2.72×10^4 degrees Kelvin and the corresponding electron neutral collision cross-section obtained from the data of Golden and Bandel¹²⁾ was 5.49 \AA^2 . The electron neutral collision frequency calculated from these values is $\nu_c = 1.20 \times 10^8 \text{sec}^{-1}$ or $\frac{\nu_c}{\omega} = 0.032$. Fig. 2 shows the impedance variation in a similar experiment performed at higher collision frequencies. The neutral gas pressure was 300 μ Hg and the corresponding collision frequency $\nu_c = 7.67 \times 10^8 \text{sec}^{-1}$ ($\frac{\nu_c}{\omega} = 0.203$); the plasma frequency was 455 MHz. Fig. 4 shows the results at the pressure of 80 μ Hg. Curve 1 is the variation in the input resistance of the antenna as the signal frequency is swept through the plasma frequency which corresponds to 290 MHz. Curve 2 shows the resistance behavior with a fixed cyclotron frequency of 182 MHz and a plasma frequency of 305 MHz. The collision frequency in this experiment was approximately $2.27 \times 10^8 \text{sec}^{-1}$; only the input resistance curves are given in this figure.

Curve 1 Fig. 4 shows the variation in antenna resistance when there is no magnetic field. The input resistance shows a pronounced maximum near $X = 1$; this peak is also predicted by Eqn. 1 when $\omega_c = 0$. In Fig. 6 the experimental resistance and conductance values shown in Fig. 1 are compared with the theoretical values of the impedance calculated from Eqn. 1 of Balmain. Figures 1, 2, 4 and 6 all show that the experimental results at the upper hybrid and cyclotron resonance conditions are in qualitative agreement with theory in that there is a peaking in the input resistance at upper hybrid resonance and in the conductance at cyclotron resonance both as predicted from Eqn. 1. The experimental values at these resonance conditions are, however, much lower than the theoretical values. Stone, Alexander and Weber⁵⁾ have also noticed that the antenna input resistance measured by them during in-flight measurements was much smaller than that calculated from Balmain's formula. This decrease and broadening of the resistance curves may be attributed to a non-collisional cyclotron damping phenomenon¹¹⁾ which has not been accounted for in Balmain's theory. The experimental curve shows an additional peak at the cut-off frequency $X = 1 - Y$ which is not accounted for by the theory; the implications of this will be considered in the next section.

IV. IMPEDANCE BEHAVIOR AT THE CUT-OFF CONDITIONS

It is interesting to note that in Fig. 4 three additional resistance peaks are observed near $X = 1$ ($P = 0$), $X = 1 - Y$ ($R = 0$) and $X = 1 + Y$ ($L = 0$) which correspond to the cut-off conditions for a loss-less magnetoplasma. The locus of the experimental parameters corresponding to Fig. 4 is shown in the CMA diagram in Fig. 5. As the signal frequency of the antenna is increased, it is seen that the locus intersects the boundary surfaces $X = 1 + Y$, $X = 1$ and $X = 1 - Y$ at the points A, B and D respectively. A distinct maxima in the input resistance near $X = 1 - Y$ when the plasma frequency is below the signal

frequency ($X < 1$) is also seen in Fig. 1; similarly a resistance peak near $X = 1 + Y$ is seen in Fig. 3, when the plasma frequency is above the signal frequency ($X > 1$).

The condition $X = 1$ corresponds to plasma cut-off. It is seen from Eqn. 1, that the $\ln \sqrt{k'/k_0}$ term causes the input impedance of the antenna to become a maximum near $X = 1$, when the plasma has significant collisional losses; the numerical calculations of Galejs indicate a peaking of resistance near the plasma cut-off.

However the theories proposed by Balmain¹⁾ and Galejs²⁾ do not predict resistance peaks near the cut-offs $X = 1 - Y$ and $X = 1 + Y$. The reason for this discrepancy will be explained in this section. Several authors^{3,4,14,15)} have indicated the branch-point singularities at the cut-off frequencies $X = 1 \pm Y$ in the Green's Function which appears as the kernel of the integral equation for the current on an antenna immersed in a magnetoplasma. Aoki³⁾ and Lee and Lo⁴⁾ have shown that as a consequence of this singularity, the axial current distribution on an infinitely long antenna in a magnetoplasma consists of two travelling current waves with different propagation constants; the interaction between these current waves can give rise to additional resonances. Lee and Lo⁴⁾ have shown that when $X < 1$ and $Y < 1$, the antenna current in the asymptotic limit of large $k_0 |z|$ is of the form:

$$I_\infty(z) = A(z)e^{-ik_0 \sqrt{k_R} |z|} + B(z)e^{-ik_0 \sqrt{k_L} |z|} \quad (3a)$$

where $k_0 = \omega \sqrt{\mu_0 \epsilon_0}$ is the free space propagation constant and:

$$k_R = 1 - \frac{XU}{U^2 - Y^2} - \frac{XY}{U^2 - Y^2} \quad \text{and} \quad k_L = 1 - \frac{XU}{U^2 - Y^2} + \frac{XY}{U^2 - Y^2} \quad (3b)$$

The amplitude coefficients $A(z)$ and $B(z)$ can be obtained from equations 23 and 24 of Lee and Lo's paper⁴⁾. In Eqns.3a and 3b, $k_0 \sqrt{k_R}$ corresponds to the

propagation constant of the right hand circularly polarized wave rotating in the same direction as the gyromotion of the electrons in the presence of the static magnetic field applied parallel to the axis of the antenna. $k_o \sqrt{k_L}$ corresponds to the left hand circularly polarized wave rotating in the opposite direction to the electronic motion or in the same direction as the positive particles. Referring to the CMA diagram given in Fig. 5, Lee and Lo have shown that in regions 1, 6 and 7 the branch cut integrations yield two propagating current waves with propagation constants equal to $k_o \sqrt{k_R}$ and $k_o \sqrt{k_L}$; in regions 2 and 3, the right-hand polarized wave becomes evanescent and there is only one propagating current wave with wave number $k_o \sqrt{k_L}$. In region 8, the left-hand polarized wave gets cut-off and there is one propagating current wave with wave number $k_o \sqrt{k_R}$. In region 5, both the current waves become evanescent.

A similar expression for antenna current has also been obtained by Aoki³⁾: when the static magnetic field is large, Aoki³⁾ has shown that the current on the infinitely long antenna is of the form:

$$I_\infty(z) = \pi \sqrt{\frac{\epsilon_o K'}{\mu}} \frac{V_o}{\Omega_z} \left(e^{-ik_o \sqrt{k_R} |z|} + e^{-ik_o \sqrt{k_L} |z|} \right) \quad (4)$$

where $K' = 1 - \frac{XU}{U^2 - Y^2}$ and V_o is the voltage of the driving generator for the antenna. $\Omega_z = \ln e^{-i\pi/2} \frac{2z}{\gamma' k_o a^2 \sqrt{K_o}}$

where $K_o = 1 - \frac{X}{U}$ and $\ln \gamma' = \gamma = 0.5772$.

The current on a finite antenna of length $2h$ can be deduced from the infinitely long antenna case, by superimposing the reflected current waves from the two ends of the antenna. Using an analysis similar to that used by Shen, King and Wu¹⁶⁾, it can be shown that the axial current on a finite antenna of length $2h$ is of the form:

$$I_h(z) = I_\infty(z) + c I_\infty(h+z) + I_\infty(h-z) \quad (5)$$

where $c = -RI_\infty(h) \frac{1}{1 + RI_\infty(2h)}$ where R is the reflection coefficient at the ends of the antenna and where $I_h(z = \pm h) = 0$. After rearranging the terms in Eqn (5) it can be shown that :

$$I_h(z) = c_0(z) e^{-ik_0 \sqrt{k_R} |z|} + c_1(z) e^{-ik_0 \sqrt{k_L} |z|} + c_2(z) \sin k_0 \sqrt{k_R} (h - |z|) + c_3(z) \sin k_0 \sqrt{k_L} (h - |z|) \quad (6)$$

where the amplitude coefficients c_0, c_1, c_2, c_3 are functions of the antenna dimensions and the plasma parameters. The method for evaluating the reflection coefficient R has been indicated by Aoki³⁾. An explicit expression for R over all ranges of the plasma parameters is difficult to obtain, so only a qualitative explanation will be given here for the presence of the resistance peaks at the cut-off frequencies. Further theoretical work on this problem is in progress now and will be reported later.

It is seen from Eqn.6 that for a loss-less plasma $k_R=0$ when $X = 1-Y$ (right cut-off) and $k_L=0$ when $X = 1+Y$ (left cut-off). Hence at these cut-off frequencies, the current on the antenna is a minimum since one of the two sine terms become zero as indicated by equations 6 and 3b. The input resistance of the antenna $R_a = \text{Re} (V/I_h(z = 0))$ goes through a maximum, when the plasma parameters correspond to the cut-off conditions. It is clear from the above discussion that the current distribution assumed by Balmain¹⁾ and the trial function for the current assumed by Galejs²⁾ are inadequate for describing the impedance behavior of the antenna at these cut-off frequencies of the magnetoplasma.

The results in Fig. 3 are particularly interesting as they show a distinct resistance peak occurring near the cut-off $X = 1 + Y$ ($L = 0$) when $\omega \ll \omega_p$ ($X > 1$). In this experiment the plasma frequency was 582 MHz and the signal frequency

was 500 MHz, so that $X = 1.345$. The electron temperature as measured by the Langmuir probe was 1.72×10^4 degrees Kelvin and the corresponding electron neutral cross-section $Q_m = 5.57 \text{ \AA}^0$. The calculated collision frequency $\nu_c = 8.76 \times 10^8$ or $\frac{\nu_c}{\omega} = 0.278$. The locus of the plasma parameters as the static magnetic field is varied as shown in Fig. 5. The resistance peaks at cut-off shown in Fig. 1 to 4 show a shift in position corresponding to the loss-less plasma case; this is due to the high collisional loss in the plasma and also partly due to slight errors in measuring the electron density with a Langmuir probe.

A comparison of Figs. 1 and 2 indicates that the resistance peak at $X = 1 - Y$ occurs only when the collisional losses are small; for large $\frac{\nu_c}{\omega}$ values the resistance peaks at $X = 1 - Y$ and at $X = 1 - Y^2$ merge to give a single, broad maximum near upper hybrid resonance. In Fig. 1, $Z = \frac{\nu_c}{\omega} = 0.032$ and the resistance maxima near $X = 1 - Y$ is clearly seen. When the collision frequency increases to $Z = 0.203$, the peak near $X = 1 - Y$ is no longer distinguishable from the one near upper hybrid resonance.

Fig. 4 shows the whole spectrum of resistance peaks which appear at the three cut-off's and at upper hybrid resonance when the signal frequency of the antenna is varied.

Similar behavior near the cut-off frequencies has also been noticed in other investigations. Cosmic noise intensity measurements¹⁷⁾ made by dipole antennas mounted on rockets and satellites also show a sharp increase in antenna resistance. This will be discussed in greater detail later in this paper.

V. IMPEDANCE BEHAVIOR AT CYCLOTRON HARMONICS

An attempt was made to determine the impedance behavior of the antenna at the second and third harmonics of the cyclotron frequency. Unfortunately for the plasma parameters corresponding to experimental results shown in Figs 1 to 4, the

second harmonic condition ($Y = 0.5$) falls in the proximity of either the upper-hybrid resonance or one of the cut-off's, so that no definite conclusion about the impedance behavior can be obtained from these results. Independent measurements, not reported here have shown that no unusual behavior was noticeable near the cyclotron second harmonic when the collision losses were high. The results shown in Fig. 1 indicate a slight increase in the input conductance of the antenna near $Y = 0.33$ which may be due to the cyclotron third harmonic. Further experimental investigation on this problem is now in progress.

VI. APPLICATIONS

a) Interpretation of maxima in cosmic noise intensity measurements

Cosmic noise intensity measurements have been made by a number of authors^{17,18)} using dipole antennas mounted on rockets and satellites. It has been shown¹⁸⁾ that the noise voltage, V_a , developed at the antenna terminals in the frequency width Δf is given by:

$$V_a^2 = 4kT_a R_a \Delta f \quad (7)$$

where R_a is the input resistance of the antenna, k is the Boltzmann's constant, and T_a is the antenna temperature. In the cosmic noise intensity measurements made by Harvey¹⁷⁾ from the UK-2 Satellite it was observed that a large increase in the noise level occurred at frequencies corresponding to $X = 1$, $X = 1 - Y$ and $X = 1 - Y^2$. The maximum noise band occupied the range $1 - Y^2 < X < 1$ and the lower limit of the noise band corresponded to a frequency at which $X = 1 + Y$. Since Eqn. 7 indicates that the noise power is directly proportional to the input resistance of the antenna, it is to be expected that a large increase in the antenna resistance should also be seen in the maximum noise band region. The results shown in Fig. 4 confirms this conclusion. It is seen that the antenna resistance is very large between $X = 1 + Y$ and $X = 1 - Y^2$ with prominent peaks

near $X = 1$, $X = 1 - Y^2$ and $X = 1 - Y$; the resistance falls off sharply below $X = 1 + Y$, indicating decreased noise levels at these lower frequencies. These results indicate that the noise intensity maxima can be directly related to the impedance behavior of the antenna near these critical frequencies.

b) Plasma resonance spikes in the ionograms of top-side sounders.

Plasma resonance spikes have been observed by Lockwood¹⁹⁾, Calvert and Goe²⁰⁾ and others in the ionograms of the Alouette Topside sounder; the frequencies at which these spikes occur are $X = 1$, $X = 1 - Y^2$, $X = 1 + Y$ and $X = 1 - Y$ and also second and higher harmonics of the cyclotron frequency. The first four resonances occur precisely at the same frequencies where resistance spikes have been noticed in our experiments. Lockwood has attributed the spikes at $X = 1 + Y$ and $X = 1 - Y$ to the propagation of the Z mode in the ionosphere.

The amplitude of these resonance spikes are, of course, dependent on the coupling between the antenna and the magnetoionic medium during transmission and reception. The space and time dependence of these resonances can be found by a Fourier integral which involves the effective impedance of the receiving antenna and Fourier transform of the transmitted pulse as has been indicated by Nuttall²¹⁾. The experimental results on the antenna impedance reported here may be useful in making quantitative calculations of the amplitude of such resonance spikes.

c) Diagnostic applications to magnetoplasmas

The resistance peak near the cut-off condition $X = 1 + Y$ which occurs when $X > 1$ ($\omega < \omega_p$) as shown in Fig. 3 and 4 is particularly interesting from a diagnostic point of view as it presents the possibility of measuring electron densities of "overdense" magnetoplasmas by using signal probing frequencies below the plasma frequency. The resonance peaks at $X = 1 - Y$ and $X = 1 - Y^2$ can

also be used for diagnostic purposes although the results are likely to be less accurate for certain ranges of the plasma parameters when these peaks appear close together.

VII. Acknowledgement

The authors thank Professor R. W. P. King for his advice and encouragement and Dr. A. D. Wunsch for several helpful discussions during the course of this investigation. The assistance rendered by Messrs. A. Cajolet and D. MacMillan in the construction of the experimental apparatus is also gratefully acknowledged.

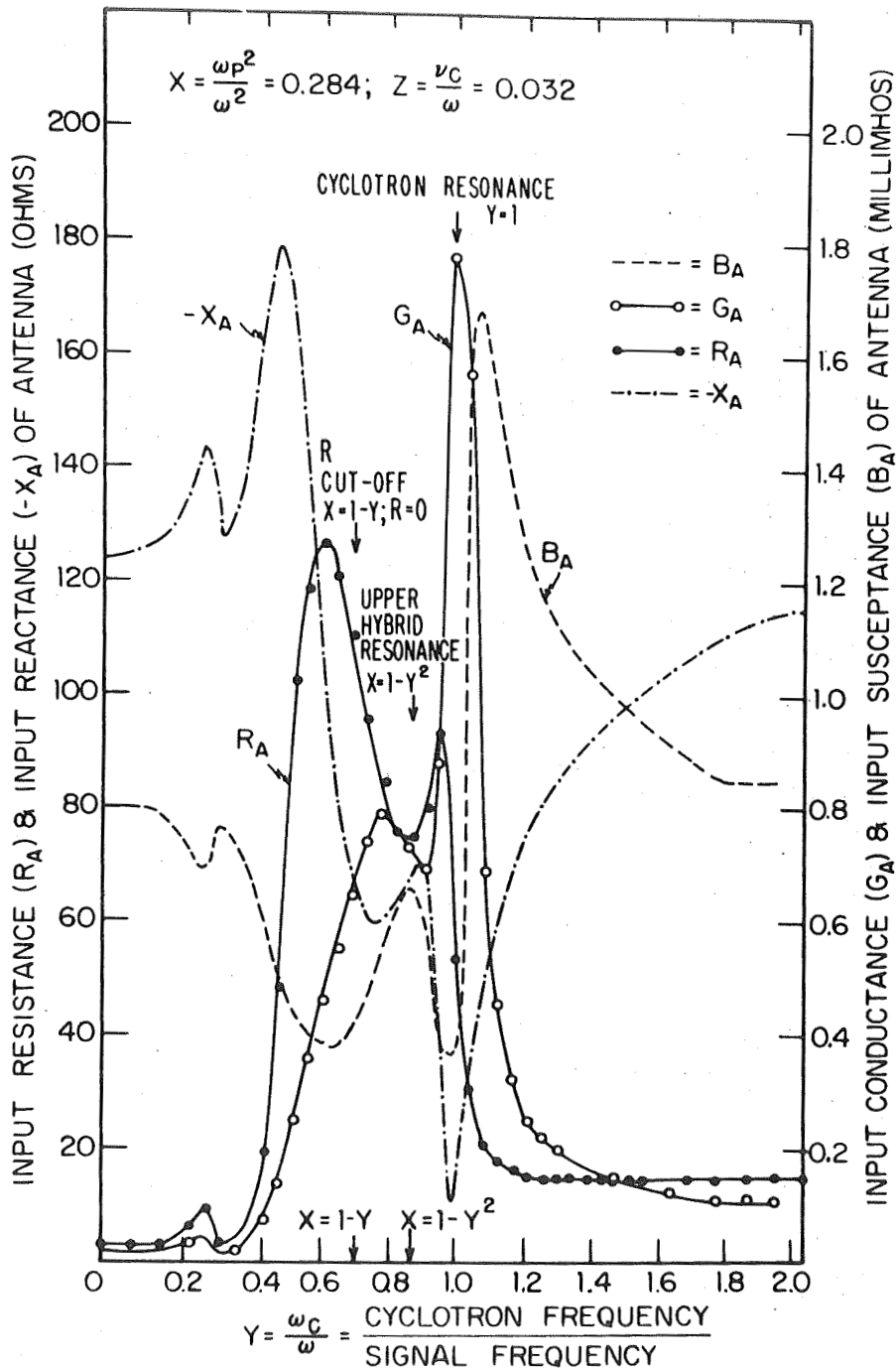


FIG. 1 IMPEDANCE OF DIPOLE ANTENNA IN A MAGNETOPLASMA. EXPERIMENTAL RESULTS; GAS-HELIUM; NEUTRAL GAS PRESSURE - $50 \mu\text{Hg}$; SIGNAL FREQUENCY = 600 MHz; PLASMA FREQUENCY = 320 MHz; $h/\lambda_0 = 0.07$; $a/\lambda_0 = 0.004$; ELECTRON TEMPERATURE = 2.72×10^4 DEGREES KELVIN.

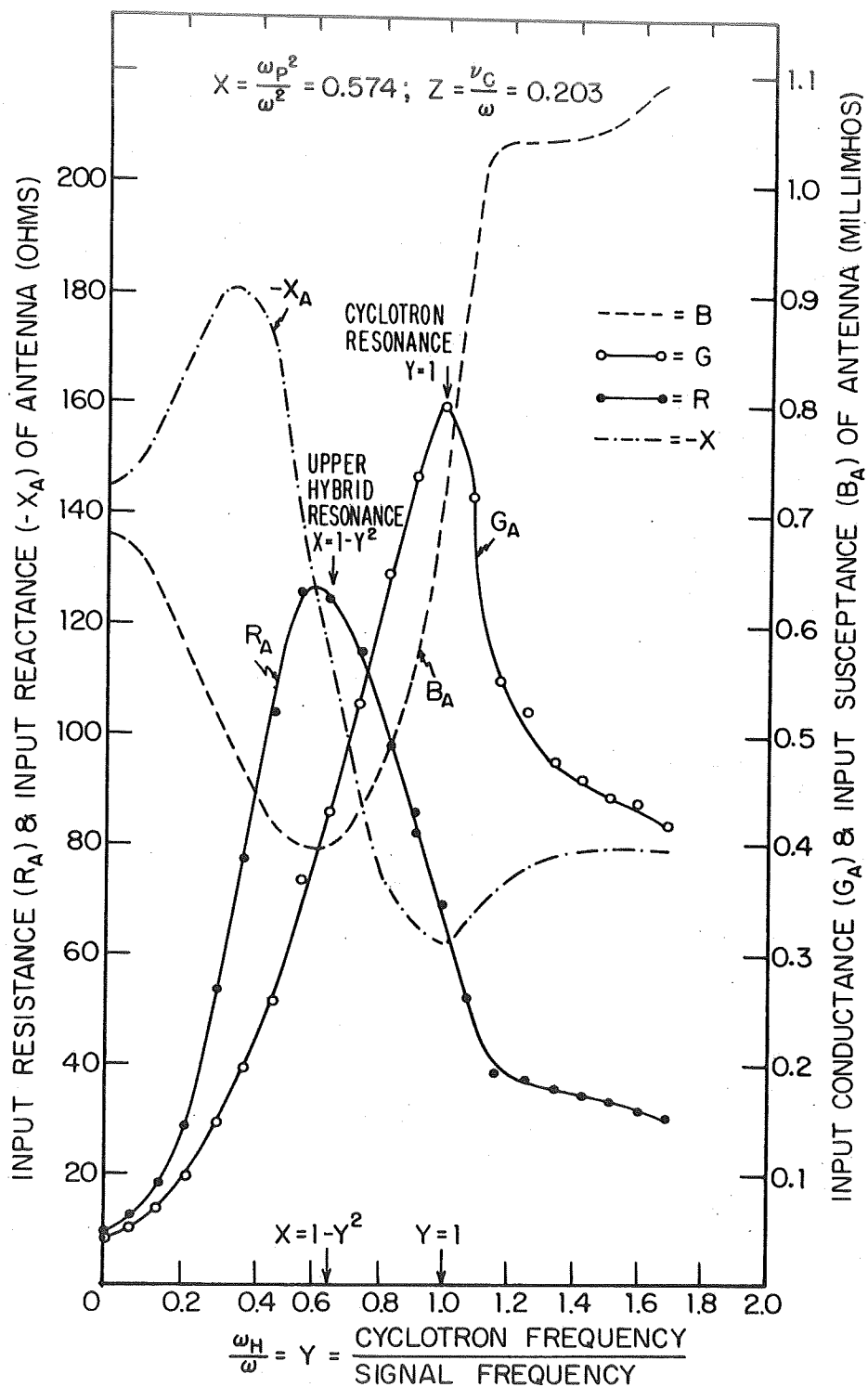


FIG. 2 IMPEDANCE OF DIPOLE ANTENNA IN A MAGNETOPLASMA EXPERIMENTAL RESULTS. GAS-HELIUM; NEUTRAL GAS PRESSURE=300 μ Hg; SIGNAL FREQUENCY=600 MHz PLASMA FREQUENCY = 455 MHz; $h/\lambda_0=0.07$; $a/\lambda_0=0.004$.

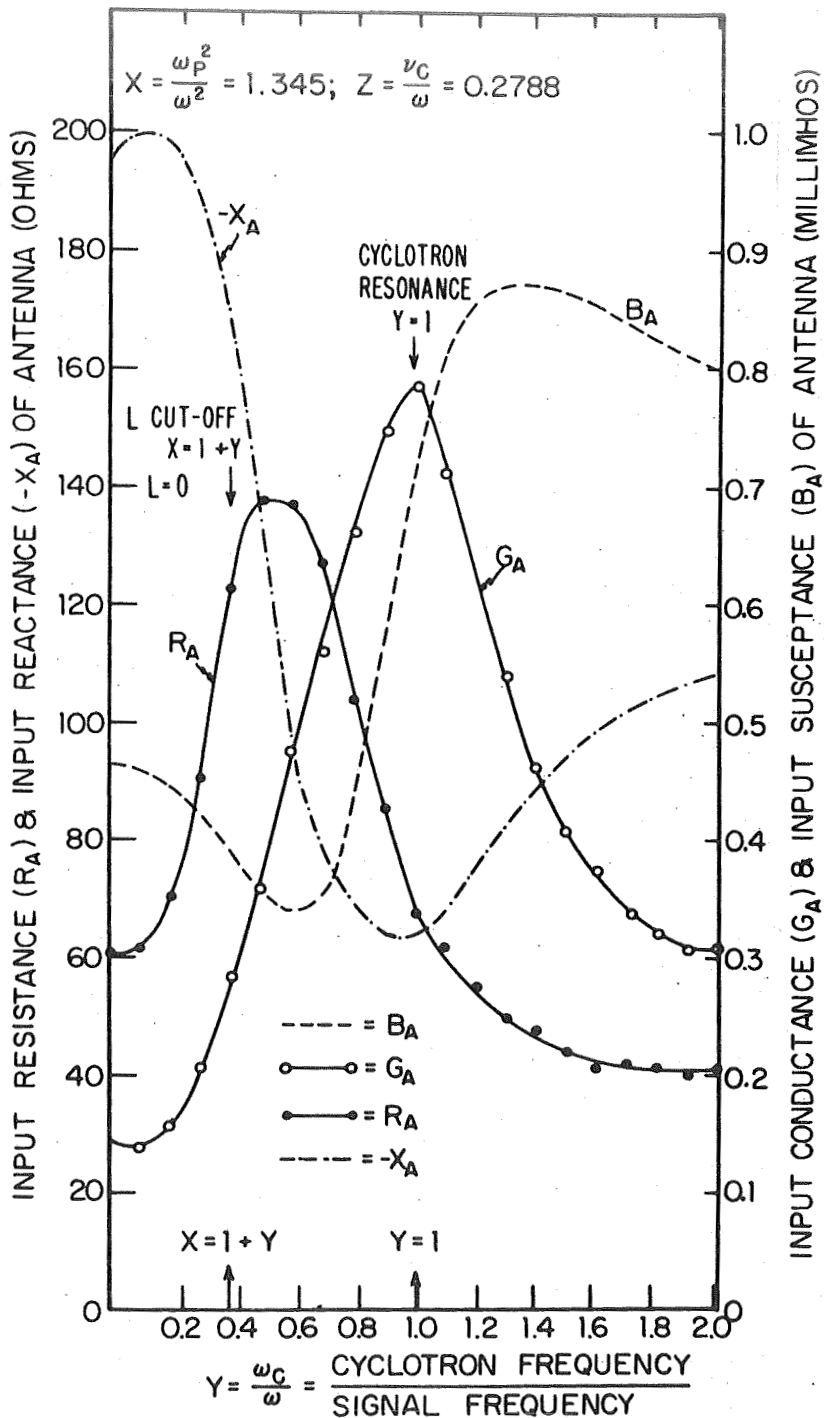


FIG. 3 IMPEDANCE OF DIPOLE ANTENNA IN A MAGNETOPLASMA. EXPERIMENTAL RESULTS. GAS-HELIUM; NEUTRAL GAS PRESSURE=450 μ Hg; SIGNAL FREQUENCY=500 MHz PLASMA FREQUENCY = 582 MHz; $h/\lambda_0=0.058$; $a/\lambda_0=0.0035$ ELECTRON TEMPERATURE = 1.72×10^4 DEGREES KELVIN.

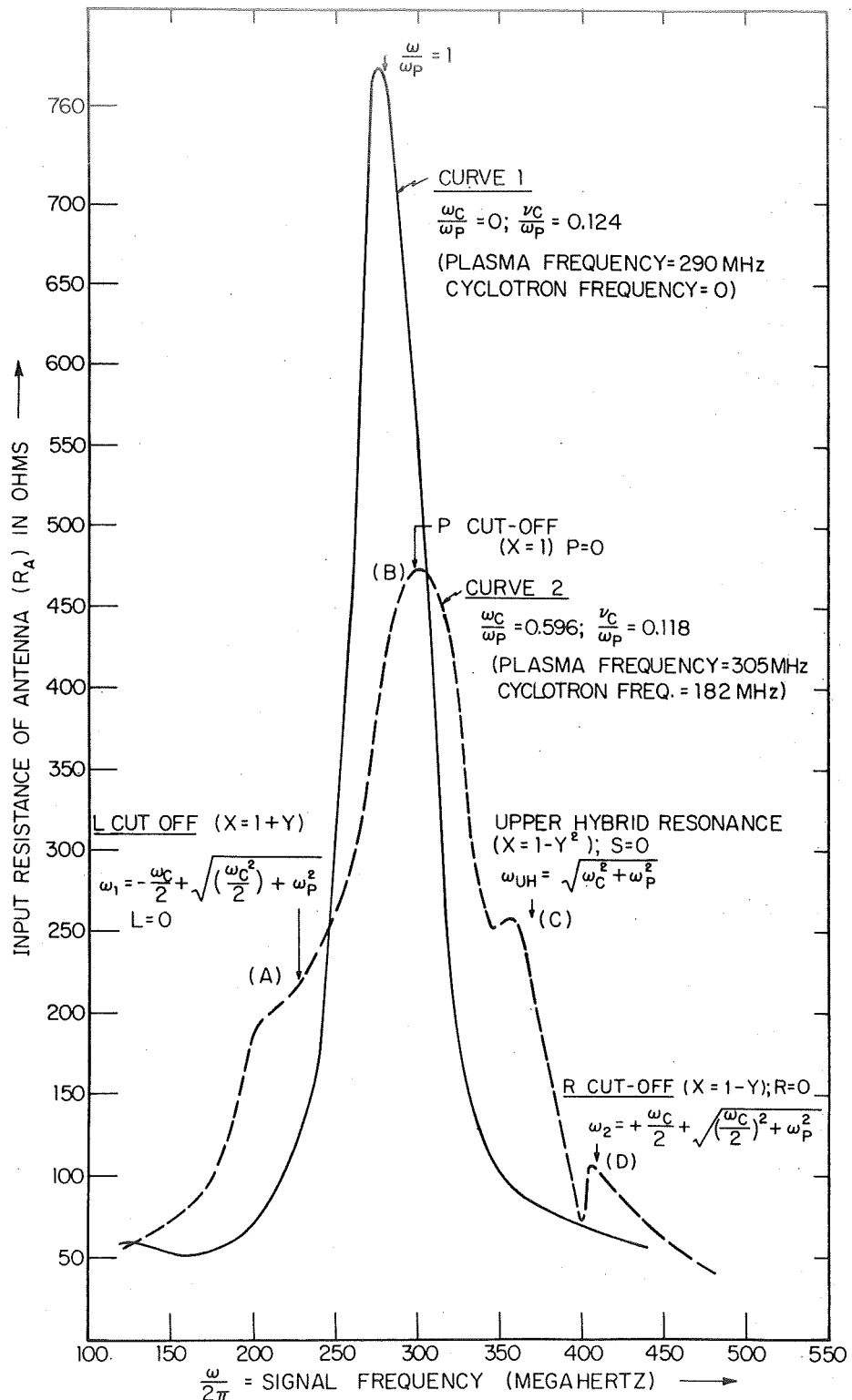


FIG. 4 IMPEDANCE OF DIPOLE ANTENNA IN A MAGNETOPLASMA - EXPERIMENTAL RESULTS. GAS-HELIUM; GAS PRESSURE = 80μ Hg; LENGTH OF ANTENNA $h = 3.49 \times 10^{-2}$ METERS RADIUS OF ANTENNA = 2.13×10^{-3} METERS CALCULATED COLLISION FREQUENCY $\nu_c = 2.27 \times 10^8 \text{ sec}^{-1}$

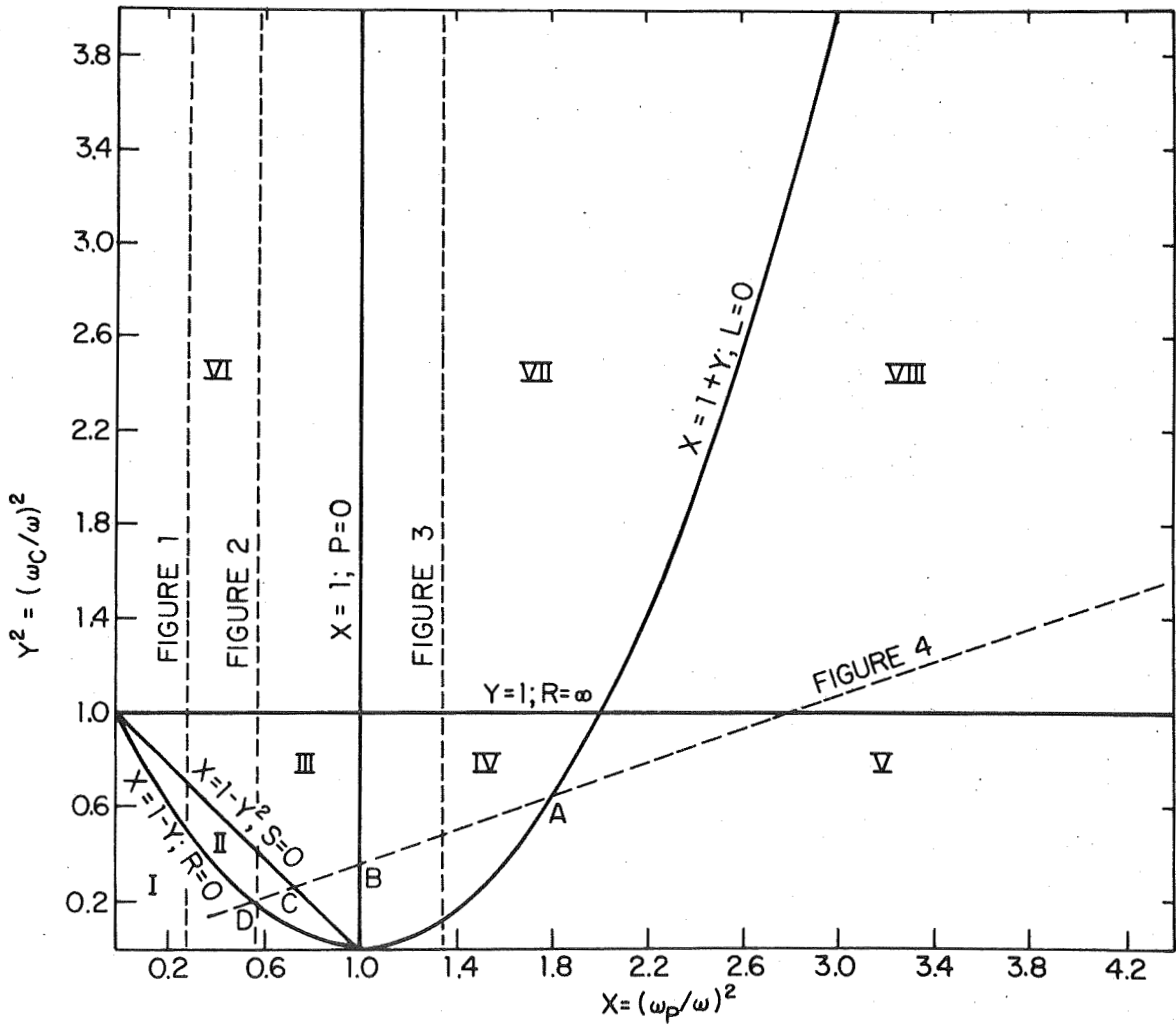


FIG. 5 THE CMA DIAGRAM WITH LOCI OF THE EXPERIMENTAL PLASMA PARAMETERS FOR FIGURES 1-4.

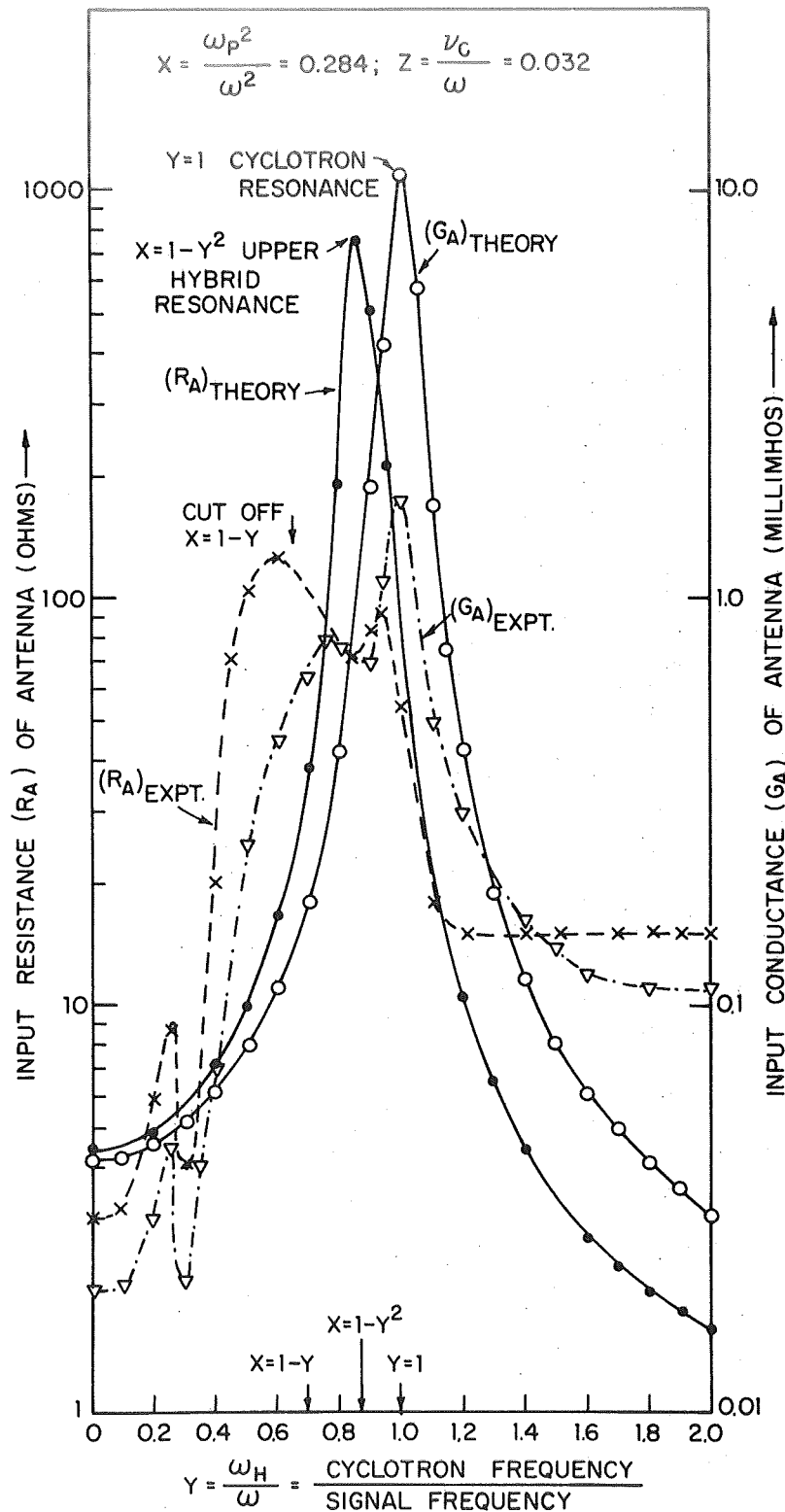


FIG. 6 COMPARISON OF EXPERIMENTAL RESULTS FOR ANTENNA IMPEDANCE WITH BALMAINS THEORY. NEUTRAL GAS PRESSURE = 50μ Hg. SIGNAL FREQUENCY = 600 MHZ PLASMA FREQUENCY = 320 MHZ

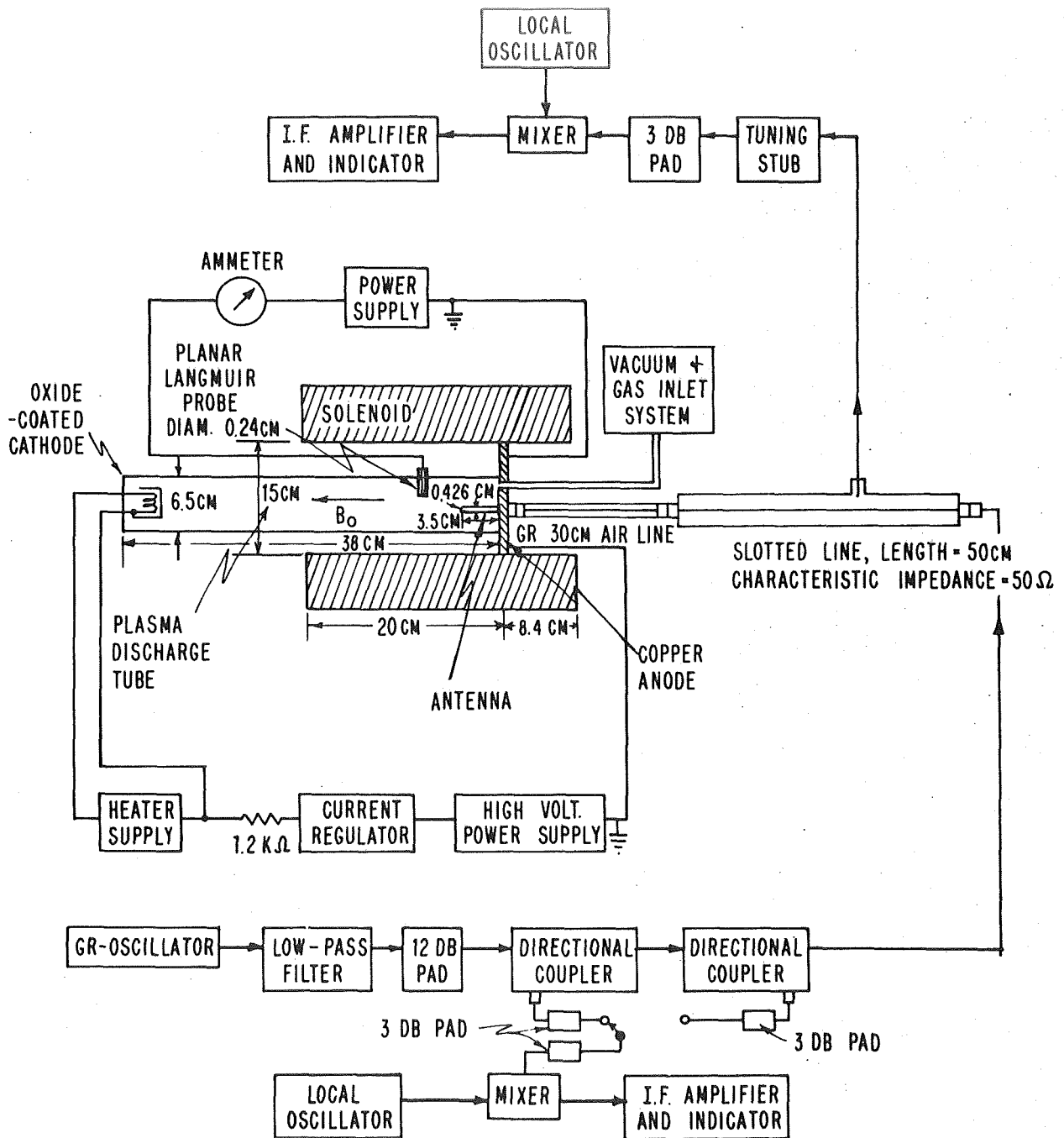


FIG. 7 BLOCK DIAGRAM OF THE EXPERIMENTAL APPARATUS

BIBLIOGRAPHY

- 1) K. G. Balmain "The Impedance of a Short Dipole Antenna in a Magnetoplasma" IEEE. Trans. on Antennas and Propagation Vol. AP-12, pp. 605-617, Sept. 1964.
- 2) J. Galejs "Impedance of a Finite Insulated Cylindrical Antenna in a Cold Plasma with a Longitudinal Magnetic Field." IEEE Trans. on Antennas and Propagation Vol. AP-14, pp. 727-736, Nov. 1966.
- 3) K. Aoki "On a Cylindrical Antenna in a Homogeneous Anisotropic Medium" Canadian Journal of Physics Vol. 44, pp. 1239-1266, 1966.
- 4) S. W. Lee and Y. T. Lo "Current Distribution and Input Impedance of an Infinite Cylindrical Antenna in Anisotropic Plasma" IEEE Trans. on Antennas and Propagation Vol. AP-15, pp. 244-252, March 1967.
- 5a) R. G. Stone, R. R. Weber and J. K. Alexander "Measurement of Antenna Impedance in the Ionosphere - I" Planet. Space Sci. Vol. 14, pp. 631-639, 1966.
- 5b) R. G. Stone, R. R. Weber and J. K. Alexander "Measurement of Antenna Impedance in the Ionosphere - II" Planet. Space Sci. Vol. 14, pp. 1007-1016, 1966.
- 6) A. R. Molozzi and J. R. Richardson "The Measured Impedance of a Dipole Antenna in the Ionosphere" Space Research VII, pp. 489-505, North Holland Publishing Company, Amsterdam.
- 7) J. Hugill "Some Measurements of Aerial Impedance in the Ionosphere" Annales D'Astrophysique pp. 255-262, No. 1, 1965.
- 8) T. H. Stix "The Theory of Plasma Waves" McGraw-Hill Book Company, 1962.
- 9) G. Francis "The Glow Discharge at Low Pressure" Handbuch Der Physik Vol. XXII - Gas Discharges II, pp. 168-175, Springer-Verlag, 1956.
- 10) R. J. Bickerton and A. Von Engel "The Positive Column in a Longitudinal Magnetic Field" Proc. Phys. Soc. Lond. Vol LXIX, 1956B, pp. 468-481.
- 11) M. A. Heald and C. B. Wharton "Plasma Diagnostics with Microwaves" Chapter 10, pp. 383-384, John Wiley & Sons, Inc. 1965.
- 12) D. E. Golden and H. W. Bandel "Absolute Total Electron-Helium-Atom Scattering Cross-sections for Low Electron Energies" Physical Review, Vol. 138, No. 1A, pp. A14-A21, April 1965.
- 13) S. R. Seshadri "Input Admittance of a Cylindrical Antenna in a Magneto-Ionic Medium" Journal of Applied Physics Vol. 39, No. 5 pp. 2407-2412, April 1968.
- 14) V. G. Davidovskii, L. V. Dubovoi and A. G. Ponomarenko "Resonance Probing of a Plasma in a Magnetic Field" Soviet Physics-Technical Physics. Vol. 9, No. 7, pp. 961-967, Jan. 1965.

- 15) J. Nuttall "Singularities of the Green's Function for a Magnetoplasma"
RCA Victor Research Report 7-801-29, Feb. 1964.
- 16) L. C. Shen, T. T. Wu and R. W. P. King "A Simple Formula of Current
in Dipole Antennas" IEEE Trans. on Antennas and Propagation Vol. AP-16,
pp. 542-547, Sept. 1968.
- 17) C. C. Harvey "Results from the UK-2 Satellite" Annales D'Astrophysique
pp. 248-254, No. 1, 1965.
- 18) D. Walsh, F. T. Haddock and H. F. Schulte "Cosmic Radio Intensities at
1.225 and 2.0 Mc. Measured up to an Altitude of 1700 km" Space Research IV,
pp. 935-958, North-Holland Publishing, Amsterdam, 1964.
- 19) G.E.K. Lockwood "Plasma and Cyclotron Spike Phenomena Observed in Top-side
Ionograms" Canadian Journal of Physics Vol. 41, pp. 190-194, 1963.
- 20) W. Calvert and G. B. Goe "Plasma Resonances in the Upper Ionosphere"
Journal of Geophysical Research Vol. 68, pp. 6113-6120, No.22, Nov. 15, 1963.
- 21) J. Nuttall "Theory of Collective Spikes Observed by the Alouette Top-side
Sounder" RCA Victor Research Report 7-801-29C pp. 12-13, April, 1964.